Proceedings World Geothermal Congress 2000
Kyushu - Tohoku, Japan, May 28 - June 10, 2000

EFFECT OF FLUID LEAKAGE AT CRACK TIP ON DYNAMICS OF FLUID-FILLED CRACK

Shin ITO[1] and Kazuo HAYASHI[2]
[1] Faculty of System Science and Technology, Akita Prefectural University, Honjyo, 015-0055, Japan
[2] Institute of Fluid Science, Tohoku University, Sendai, 980-8577, Japan

Key Words: geothermal reservoir crack, fluid leakage, dynamic response, HDR, HWR

ABSTRACT

Dynamic response of a reservoir crack with fluid leakage along the crack periphery is studied by using a two-dimensional fluid-filled crack in an elastic medium, i.e. a rock mass. In order to understand the source mechanism of microseismic events observed during hydro fracturing, many crack models were constructed and were analyzed. Those crack models were made up of an infinite fluid-filled slit or a single crack. However, in HDR/HWR fields, geothermal reservoirs consist of networks of cracks and permeable layers. This means that fluid leakage from the crack tip likely to be one of the main parameters governing the dynamics of a fluid-filled crack. A simple model is constructed to examine how the fluid leakage at the crack tip affects the dynamics of the crack, where we take account of the effect of fluid viscosity, permeability of rock and interfacial stiffness due to contact between the asperities on the upper and lower surfaces of the crack. We model the fluid leakage from the crack tip to be one-dimensional fluid flow in the direction along the extension line of the crack and express a variety of fluid leakage phenomena by introducing an appropriate boundary condition for fluid motion at the crack tip. We use Darcy's law for describing fluid leakage at the crack tip. We derive a singular integral equation for determining the displacement gap across the crack in the Laplace image and Fourier image spaces, where the motion of fluid in the crack is taken into account, and we solve the integral equation numerically. It is revealed that fluid leakage has strong effect on the higher modes of oscillation. The eigen angular frequencies become smaller with increasing fluid leakage at the crack tip. Nodes of each mode of oscillation approach the crack tip with increasing fluid leakage. It is also revealed that intensity of attenuation becomes stronger with increasing fluid leakage. However, for fluid leakage exceeding a certain value, the situation is opposite, i.e., attenuation becomes weaker with increasing fluid leakage. These effects of fluid leakage at the crack tip are stronger for the larger interfacial stiffness along the crack line and weaker for larger fluid viscosity and for larger aspect ratio, i.e. the ratio of the crack length to the initial aperture of the crack.

1. INTRODUCTION

In the advanced geothermal heat extraction such as HDR (Duchane, 1991) and HWR (Takahashi and Hashida, 1992), one of the key technologies is the characterization of geothermal reservoir cracks created by hydraulic fracturing. It is critical if we can estimate the basic geometrical characteristics, such as size, aperture and degree of contact between the upper and lower crack surfaces. For this purpose, AE/MS methods are most promising. The so-called passive acoustic methods have been verified to be powerful in the characterization (Niitsuma et al., 1987) and have been widely used (e.g., Fehler and Bame, 1985). In the passive acoustic methods, elastic waves due to crack growth during hydraulic fracturing are monitored to estimate the geometrical and mechanical characteristics of reservoir cracks. In order to estimate the characteristics of a reservoir crack, we first need to understand the dynamic response of a fluid-filled crack. So far the dynamic response of a fluid-filled crack has received fairly intensive attentions for understanding the source mechanism of volcanic earthquakes and microseismic events observed during hydraulic fracturing (Chouet, 1986; Ferrazzini and Aki, 1987; Dvorkin et al., 1992). Ferrazzini et al. (1990) examined the field AE data observed at Fenton Hill (US HDR test site) and estimated the characteristics of the reservoir cracks. Those models just stated above employed an infinite fluid-filled slit or a single crack surrounded by impermeable or permeable rock. However, in HDR/HWR fields, geothermal reservoirs consist of networks of cracks and permeable layers. Furthermore, microseismic events during massive hydraulic fracturing occur primarily on or close to preexisting faults or joints. These two points suggest that fluid leakage from the crack tip likely to be one of the main parameters governing the dynamics of a fluid-filled crack.

In the present paper, we study the dynamic response of a two-dimensional fluid-filled crack in an elastic medium in order to clarify the basic characteristics of dynamics of a reservoir crack, paying special attention to examine how the fluid leakage from the crack tip affects the dynamics of the crack. We also take account of the effect of fluid viscosity, permeability of rock and interfacial stiffness due to partial contact between the asperities on the upper and lower crack surface, as well. We model the fluid leakage from the crack tip to be one-dimensional flow in the direction along the extension line of the crack and express a variety of fluid leakage phenomena by introducing an appropriate boundary condition for fluid motion at the crack tip. Regarding fluid dynamics in the crack, we follow the approach employed by Dvorkin et al. (1990). Firstly, we derive a singular integral equation defined along the crack line in the Laplace and Fourier image spaces and solve it numerically. Then we discuss the effect of the fluid

leakage on the dynamic response of the crack.

2. CRACK MODEL

Let us consider an oscillating two-dimensional fluid-filled crack of length $2a$ and of aperture d in an infinite elastic medium (Figure 1). Let us introduce a Cartesian coordinate system x_i (i=1, 2, 3). The stress and the displacement, referred to the coordinate system, are denoted as σ_{ij} and u_i (i, j =1, 2, 3), respectively. The fluid leakage from the crack tip is assumed to be one-dimensional flow in the direction along the extension line of the crack. The permeable layer on which crack exists is saturated with fluid. The permeability of the layer is significantly small compared to the crack itself but is large enough compared to the intact rock. Through the crack surface, fluid filtrates into the surrounding permeable rock. In the following, the stiffness per unit area induced by the partial contact between the upper and lower crack surfaces is denoted as k. We call the stiffness "interfacial stiffness". Let C_L and C_T be the phase velocities of the P and S waves of the rock. Let $\overline{g}(p)$ be the Laplace transform of a function $g(t)$ of time t. The boundary condition on the crack surface is expressed as follows:

$$\overline{\sigma}_{33}\,|_{x_3\to+0} = k\Delta\overline{u}_3 - \overline{P} + \overline{\sigma}^*_{33} \qquad (|x_1| < a), \tag{1}$$

where Δu_3 is the gap of u_3 induced along the crack line, P is the pressure of the fluid in the crack and σ^*_{33} is the normal stress applied to the crack surface. Following Hayashi et al. (1995), we finally arrive at the following expression for the stress $\overline{\sigma}_{33}$ on the crack surface after tedious manipulations:

$$\begin{aligned}
&\overline{\sigma}_{33}(x_1, x_3, p)\big|_{x_3\to+0} \\
&= \frac{\mu}{2\pi}\,\mathbf{Pf}\int_{-a}^{+a}\Delta\overline{u}_3(\xi_1, p) \\
&\times\left[q_1\frac{p}{C_T\zeta}K_1\left(\frac{p\zeta}{C_T}\right) - q_2\frac{p^2}{C_T^2}K_2\left(\frac{p\zeta}{C_T}\right)\right. \\
&+ q_3\frac{1}{\zeta^2}\left\{K_2\left(\frac{p\zeta}{C_T}\right) - \frac{1}{\kappa^2}K_2\left(\frac{p\zeta}{C_L}\right)\right\} \\
&- q_4\frac{p}{C_T\zeta}\left\{K_3\left(\frac{p\zeta}{C_T}\right) - \frac{1}{\kappa^3}K_3\left(\frac{p\zeta}{C_L}\right)\right\} \\
&\left.+ q_5\frac{p^2}{C_T^2}\left\{K_4\left(\frac{p\zeta}{C_T}\right) - \frac{1}{\kappa^4}K_4\left(\frac{p\zeta}{C_L}\right)\right\}\right] d\xi_1\,, \\
&\qquad (|x_1| < a).
\end{aligned} \tag{2}$$

Here, μ is the shear modulus of the medium, κ=C_L/C_T and ζ=$|x_1-\xi_1|$. The symbol $\mathbf{Pf}\int$ denotes the finite part integral. Coefficients q_1~q_5 are known functions of κ, the expressions of which are not presented here for brevity.

Let us assume that the amplitude of oscillation of the crack surface is small compared to the original aperture of the crack and that the variation of the fluid density is much smaller than its reference undisturbed value. Following Dvorkin et al. (1990), we finally arrive at the following differential equation for the fluid pressure $\overline{P}$ in the Laplace image space:

$$\begin{aligned}
&\frac{1}{\overline{n}_f^2\eta}\left\{\frac{1}{\overline{n}_f}\tanh\left(\frac{\overline{n}_f d}{2}\right) - \frac{d}{2}\right\}\frac{\partial^2\overline{P}}{\partial x_1^2} \\
&\quad + \left\{\sqrt{\frac{pm_0k_0}{b\eta}} + \frac{d}{2}\frac{p}{b}\right\}\overline{P} = -\frac{p}{2}\Delta\overline{u}_3\,,
\end{aligned} \tag{3}$$

where

$$\overline{n}_f = \sqrt{\frac{\rho_f p}{\eta}}\,. \tag{4}$$

Here, η is the fluid viscosity, m_0 is the porosity of the surrounding rock, k_0 is the permeability of the rock, b is the bulk modulus of the fluid and ρ_f is the density of the fluid. We impose the boundary condition that, at the crack tip, the fluid velocity u_{f1} in the x_1-direction inside the crack is equal to the sum of the velocity in the x_1-direction of the elastic medium and the fluid velocity of fluid leakage. Then the boundary condition at the crack tip is expressed as follows:

$$\overline{u}_{f1}\big|_{x_1=a} = p\overline{u}_1\big|_{x_1=a} + \sqrt{\frac{m_l k_l p}{\eta b}}\,\overline{P}\big|_{x_1=a}\,, \tag{5}$$

where, m_l and k_l are the porosity and the permeability of the permeable layer respectively. Second term in the right hand side of eq.(5) can be derived from Darcy's law and the conservation of mass in the permeable layer under the condition that the pressure is continuous across the crack tip into the x_1-direction and the pressure is undisturbed far from the crack tip. In order to perform numerical calculations, we need values of m_l and k_l. Since we do not know these values in real fields, we replace the permeable layer by a slit with equivalent hydraulic properties (Figure 2). The aperture of the slit with equivalent hydraulic properties is denoted d_l, and we call this aperture "the effective aperture". We set m_l=d_l/d and k_l=d_l^2/12.

Let us introduce the following non-dimensional quantities:

$$x = \frac{x_1}{a}\,,\quad s = \frac{ap}{C_T}\,,\quad \delta_0 = \frac{ak}{\mu}\,,\quad \overline{\phi}(x,s) = \frac{C_T\Delta\overline{u}_3(x_1,p)}{a^2}\,. \tag{6}$$

By substituting eq.(2) into eq.(1) and also the expression of $\overline{P}$ derived from eq.(3) into eq.(1), we get a singular integral equation of the non-dimensional displacement gap $\overline{\phi}$. By taking account of the asymptotic behavior of the displacement gap at the crack tip, let us express the non-dimensional displacement gap as follows, with unknown coefficients $\overline{A}_n$ and the Chebyshev polynomial of the second kind $U_n(\cdot)$:

$$\overline{\phi}(x,s) = \sqrt{1-x^2}\sum_{k=1}^{N}\overline{A}_k(s)U_k(x)\,. \tag{7}$$

By substituting eq.(7) into the singular integral equation and by

applying a usual collocation technique, we finally arrive at the simultaneous linear algebraic equations for $\overline{A}_n$ (n=1, 2, …, N). Let us introduce a function $\Delta(s)$, which is determinant of the matrix, the elements of which are the coefficients of the simultaneous linear algebraic equations. The imaginary parts of the roots of $\Delta(s)$=0 are the eigen angular frequencies and the real parts of the roots of $\Delta(s)$=0 represent the intensity of the attenuation of the oscillation. In the following, we denote the roots of $\Delta(s)$=0 as α_j. Here, j represents the mode number of the oscillation. It should be noted that the complex conjugate of α_j is also the root of $\Delta(s)$=0 and $s=\alpha_j$ is the zero point of order 1. By performing the inverse Laplace transform, we arrived at the following expression for the non-dimensional displacement gap across the crack:

$$\left.\begin{aligned}\phi(x,\tau) &= \sum_{j=1}^{\infty}\phi_j(x,\tau)\\ \phi_j(x,\tau) &= \sqrt{1-x^2}\sum_{k=1}^{N}\mathrm{Re.}\left\{B_k(\alpha_j)\cdot e^{\alpha_j\tau}\right\}U_k(x)\end{aligned}\right\}, \tag{8}$$

where τ is non-dimensional time defined as $\tau=C_T t/a$ and B_k is function of α_j.

Following Hayashi et al. (1995), we define the non-dimensional interfacial stiffness δ_0 such that

$$\delta_0 = \delta_0' \frac{a/d}{\sqrt{1-x^2}}, \tag{9}$$

where

$$\delta_0' = 2(1+\nu)\frac{A^*}{A_0}. \tag{10}$$

Here, ν is the Poisson's ratio of elastic medium, A_0 is the crack area and A^* is the real contact area on the crack area.

The dynamic response of a two-dimensional fluid-filled crack is analyzed also in the Fourier image space. The resulting expressions are obtained readily by replacing the parameter p into $-i\omega$ in the expressions for the Laplace image space, where ω is angular frequency. In the following, we introduce a parameter Ω and a function $\tilde{\phi}(x,\Omega)$. The parameter Ω is defined as $\Omega=a\omega/C_T$. The function $\tilde{\phi}(x,\Omega)$ is the Fourier transform of a function $\phi(x,\tau)$.

3. DYNAMIC RESPONSE OF THE CRACK

Following values have been used, referring the material properties of water and granite: the ratio of the rock density to fluid density is 2.5, μ/b=15, ν=0.25 (κ=1.7), m_0=0.01, k_0=10^{-19}m^2. Also, we have set the aspect ratio a/d to be 10^3, 5×10^3, 10^4, aperture d to be 10^{-4}, 10^{-3}, 10^{-2}m, the interfacial stiffness δ_0' to be 0, 0.01, 0.1 and fluid viscosity η to be 10^{-3}, 10^{-2}, 2×10^{-2} Pa·s (1~20cP). Here, we call the ratio of the effective aperture d_l to the initial aperture d "aperture ratio" and have set the aperture ratio to be 10^{-3}, 10^{-2}, 10^{-1}. Large aperture ratio means large fluid leakage.

Figure 3 shows examples of spectra of non-dimensional displacement gap across the crack $\tilde{\phi}(x,\Omega)$. Dark shade in Figure 3 means large displacement gap across the crack $\tilde{\phi}(x,\Omega)$. The oscillation of the crack surface has the modes with total node number 1, 2, 3,··· (Figure 3). We call, in the following, these modes the 2nd, 3rd, 4th,··· modes, respectively. The numbers between two figures indicate the mode numbers. Eigen angular frequencies are smaller for larger aperture ratios, as is discussed later in detail. Especially, effect of the leakage is stronger on the higher modes than on the lower modes and nodes become unclear with increasing aperture ratio. Figure 4 shows waveforms of the 5th mode. Nodes near the crack tip approach the crack tip with increasing fluid leakage. Peaks between the crack tip and the node near the crack tip become lower with increasing fluid leakage and vanish for large fluid leakage. Figure 5 shows variation of non-dimensional eigen angular frequencies with respect to aperture ratio. In this figure, the results shown on the extreme left are the results obtained under the boundary condition that there is no fluid leakage at the crack tip. In this case, the second term of the left hand side in eq.(5) is absent. We call this boundary condition "close condition". The results shown on the extreme right are the results obtained under the boundary condition that fluid in the crack goes in and out completely freely across the crack tip. In this case, instead of eq.(5), we use the boundary condition that pressure caused by oscillation is equal to zero (P=0) at the crack tip. We call this condition "open condition". Eigen angular frequencies of close condition and those of low fluid leakage are almost the same. For large fluid leakage, the eigen angular frequency of the Nth mode is almost the same as that of the (N-2)th mode derived under open condition. This result can be derived from Figure 4. Since nodes near the crack tip approach to the crack tip with increasing fluid leakage in Figure 4, the Nth mode of closed condition changes into the (N-2)th mode of open condition. Eigen angular frequency of the 2nd mode becomes smaller with increasing fluid leakage. Figure 6 shows the effect of aperture and the interfacial stiffness on eigen angular frequencies of the 3rd and 4th modes. In Figure 6(a), when the interfacial stiffness is zero, i.e., when the crack is completely open up without any partial contact, effect of fluid leakage is weak. In Figure 6(b), when the interfacial stiffness is large, effect of fluid leakage is strong. Especially, effect of fluid leakage is stronger for large aperture. Figure 7 shows the effect of aspect ratio on eigen angular frequencies of the 3rd and 4th modes. Effect of fluid leakage is

stronger for smaller aspect ratio. Figure 8 shows the effect of fluid viscosity on eigen angular frequencies of the 3rd and 4th modes. Effect of fluid leakage is weaker for larger fluid viscosity. Now we introduce a non-dimensional parameter L defined as

$$L = \frac{m_l k_l}{d^2} d \frac{1}{a/d} \frac{1}{\eta / \rho_f} C_T . \qquad (11)$$

This parameter L is derived from the second term in the right hand side of eq.(5). From the results shown in Figures 6, 7 and 8, fluid leakage at the crack tip disturbs the oscillation of the crack more strongly for larger aperture d, smaller aspect ratio a/d and smaller fluid leakage η. By combination of these parameters, the parameter L becomes large. Except for the effect of the interfacial stiffness, we can explain the effects of these parameters on the oscillation of crack by using the parameter L. When the parameter L is large enough, oscillation of crack under close boundary condition at the crack tip changes to oscillation of crack under open boundary condition. Figure 9 shows variation of intensity of attenuation of the 3rd and 7th modes with respect to aperture ratio. Larger value of |Re. α_j| means larger intensity of attenuation (see eq.(8)). The intensity of attenuation becomes larger with increasing aperture ratio at smaller aperture ratio and then switches to become smaller with increasing aperture ratio at larger aperture ratio. As a result of increasing fluid leakage, intensity of attenuation of the Nth mode under close condition becomes intensity of attenuation of the (N-2)th mode under open condition.

4. CONCLUSIONS

The dynamic response of a two-dimensional fluid-filled crack was examined, emphasizing the effects of fluid leakage at the crack tip, the interfacial stiffness, aperture, aspect ratio of the crack and fluid viscosity. We adopted Darcy's law for describing fluid leakage at the crack tip. The conclusions that are derived from the present work can be summarized as follows:

(1) For larger fluid leakage at the crack tip, non-dimensional eigen angular frequency is smaller than that for no fluid leakage. Waveform of the Nth mode of close boundary condition at the crack tip changes to the waveform of the (N-2)th mode of open boundary condition with increasing fluid leakage.
(2) The effect of fluid leakage at the crack tip is strong for the higher mode, the larger interfacial stiffness, larger aperture, smaller aspect ratio and smaller fluid viscosity.
(3) The intensity of attenuation becomes larger with increasing fluid leakage at smaller fluid leakage and then switches to become smaller with increasing fluid leakage at larger fluid leakage.

ACKNOWLEDGMENTS

The authors wish to thank Mr. K. Kuroki for his help in preparing for the paper. The present work was supported by NEDO (New Energy and Industrial Technology Development Organization) under International Joint Research Grant "Murphy Project".

REFERENCES

Chouet, B. (1986). Dynamics of a Fluid-Driven Crack in Three Dimensions by the Finite Difference Method. *J. Geophys. Res.*, 91, pp.13967-13992.

Duchane, D. (1991). International Programs in Hot Dry Rock Technology Development. *Geother. Resour. Coun. Bull.,* 20, pp.135-142.

Dvorkin, J., Mavko, G. and Nur, A. (1990). The Oscillations of a Viscous Compressible Fluid in an Arbitrarily-Shaped Pore. *Mechanics of Materials*, 9, pp.165-179.

Dvorkin, J., Mavko, G. and Nur, A. (1992). The Dynamics of Viscous Compressible Fluid in a Fracture. *Geophys.*, 57, pp.720-726.

Fehler, M. and Bame, D. (1985). Characteristics of Microearthquakes Accompanying Hydraulic Fracturing as Determined from Studies of Spectra of Seismic Waveforms. *Geother. Resour. Coun. Trans.*, 9-II, pp.11-16.

Ferrazzini, V. and Aki, K. (1987). Slow Waves Trapped in a Fluid-Filled Infinite Crack: Implication for Volcanic Tremor. *J. Geophys. Res.*, 92, pp.9215-9223.

Ferrazzini, V. Chouet, B., Fehler, M. and Aki, K. (1990). Quantitative Analysis of Long-Period Events Recorded during Hydrofracture Experiments at Fenton Hill, New Mexico. *J. Geophys. Res.*, 95, pp.21871-21884.

Hayashi, K., Niiyama, K. and Abé, H. (1995). Dynamic Response of a Rock Mass with a Large Fluid-Filled Crack. *Mechanics of Jointed and Faulted Rock, ed., Rossmanith, H. P., Balkema,* pp.699-705.

Niitsuma H., Chubachi, N. and Takanohashi, M. (1987). Acoustic Emission Analysis of Geothermal Reservoir and its Application to Reservoir Control. *Geothermics*, 16, pp.47-60.

Takahashi, H. and Hashida, T. (1992). New Project for Hot Wet Rock Geothermal Reservoir Design Concept. *Proc. 17th Stanford workshop on geothermal reservoir engineering, Stanford,* pp.39-44.

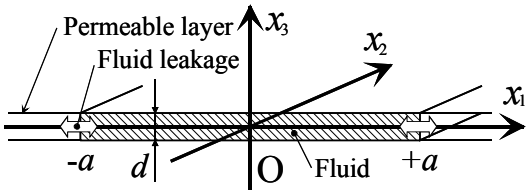

Figure 1. Coordinate system and a two-dimensional fluid-filled crack (hatched) with fluid leakage at the crack tips.

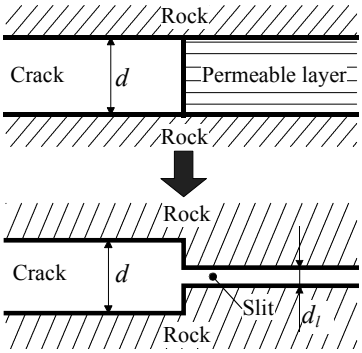

Figure 2. Model of permeable layer.

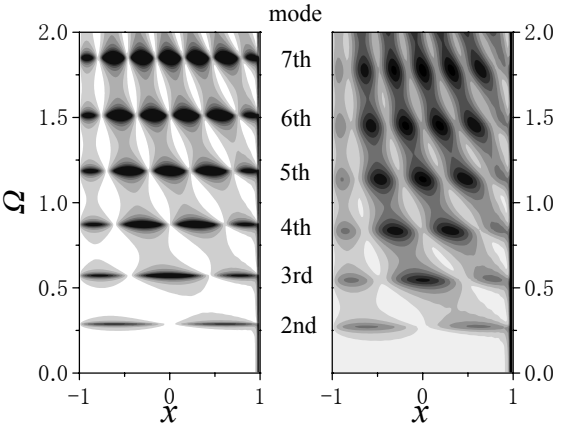

(a) $d_l/d=10^{-3}$ (b) $d_l/d=10^{-1}$

Figure 3. Examples of spectra of non-dimensional displacement gap across the crack ($a/d=10^3$, $\delta_0'=0.01$, $\eta=10^{-3}$ Pa·s, $d=10^{-3}$m).

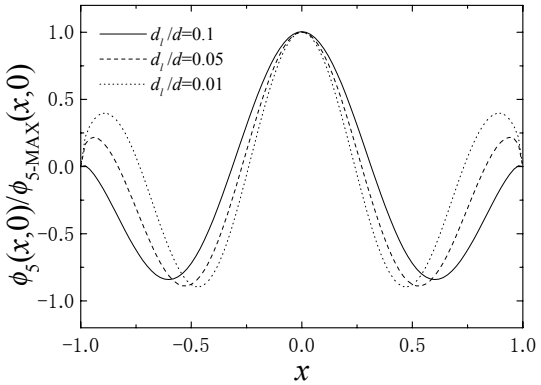

Figure 4. Waveforms of the 5th mode ($a/d=10^3$, $\delta_0'=0.1$, $\eta=10^{-3}$ Pa·s, $d=10^{-2}$m).

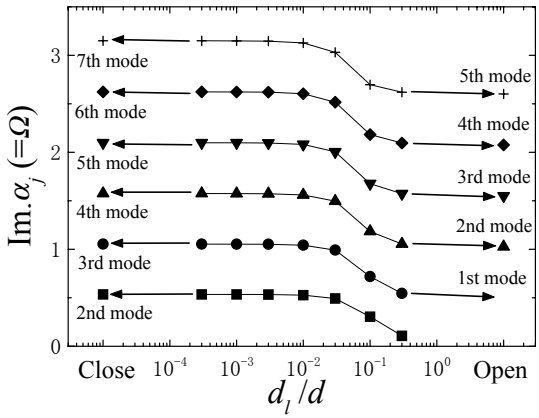

Figure 5. Variation of non-dimensional eigen angular frequencies with respect to aperture ratio ($a/d=10^3$, $\delta_0'=0.1$, $\eta=10^{-3}$ Pa·s, $d=10^{-2}$m).

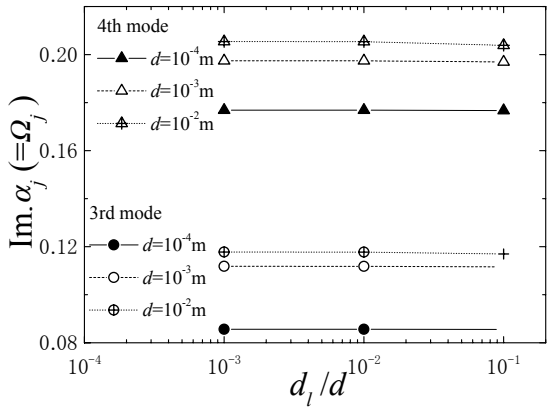

(a) $\delta_0'=0.0$

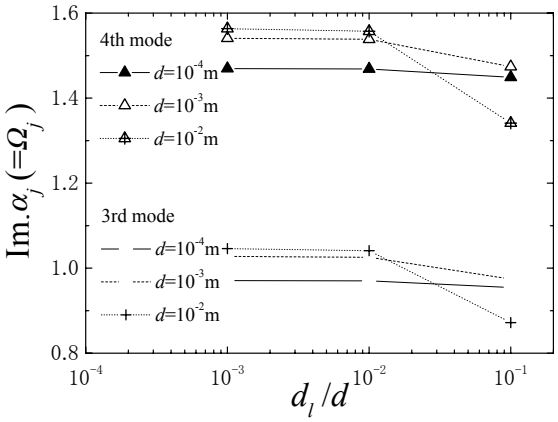

(b) $\delta_0'=0.1$

Figure 6. Effect of aperture and interfacial stiffness on non-dimensional eigen angular frequencies of the 3rd and 4th modes ($a/d=5\times10^3$, $\eta=10^{-3}$ Pa·s).

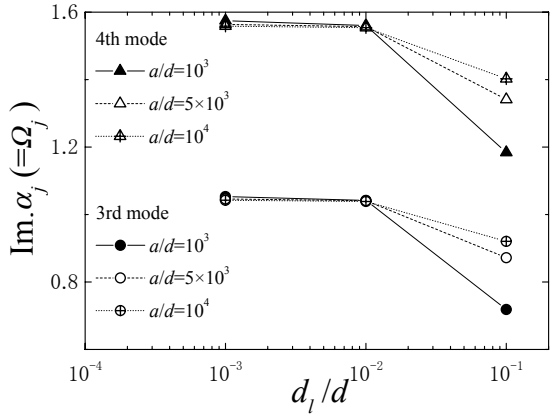

Figure 7. Effect of aspect ratio on non-dimensional eigen angular frequencies of the 3rd and 4th modes (δ_0'=0.1, η=10^{-3} Pa·s, d=10^{-2}m).

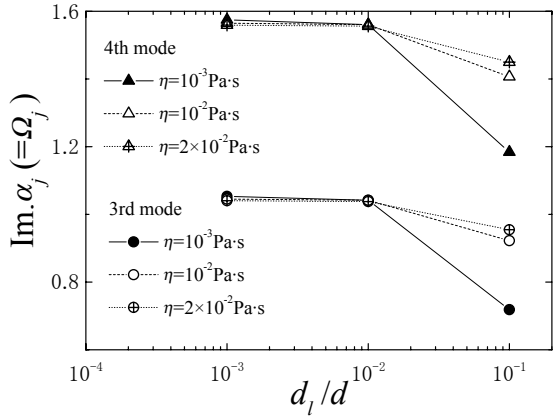

Figure 8. Effect of fluid viscosity on non-dimensional eigen angular frequencies of the 3rd and 4th modes (a/d=10^3, δ_0'=0.1, d=10^{-2}m).

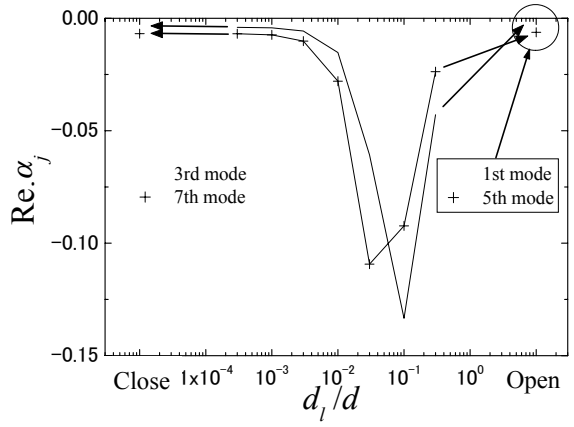

Figure 9. Variation of intensity of attenuation of the 3rd and 7th modes (close boundary condition at crack tip) with respect to aperture ratio (a/d=10^3, δ_0'=0.1, η=10^{-3} Pa·s, d=10^{-2}m).